Archive of Applied Mechanics (2025) 95:252
https://doi.org/10.1007/s00419-025-02959-5

ORIGINAL

N. Ghiasi · P. Sharma · A. Jung · S. Diebels

Modelling the electrodeposition of nickel on polyurethane foam

Received: 27 December 2024 / Accepted: 5 October 2025 / Published online: 17 October 2025

Abstract The electrodeposition method is among the various methods to produce metal foams by coating open-cell polymeric foams with a metallic layer. This process is governed by strong mechanical and electrical interactions which arise due to different factors such as presence of ions in the electrolyte, applied external current, charged solid surface and ionic concentration gradient. Hence, the related physical effects result in a nonlinear coupled process at the macroscale, which introduces a complex challenge for modelling and computational treatment. This work proposes a model to describe the electrocoating of polyurethane foams with nickel ions at macroscale, in an isothermal process and under the simplifying assumptions such as rigidity of the foam and incompressibility of the electrolyte. To do so, the multi-phase flow through the porous medium has to be modelled on a macroscopic scale. The governing equations describing the coating process are developed from the fundamental balance equations of mixture theory. By reasonable physical assumptions, different processes contributing to ionic transport, i.e. diffusion, convection and migration, are considered, and finally, the influence of different parameters in each transport mechanism is investigated. First 1D simulations show that the presented model is able to describe the experimentally observed effects, at least in a qualitative way.

Keywords Hybrid metal foams · Ni/Pu foams · Double-sided modelling · Mixture theory

1 Introduction

Porous materials or foams are continuously interconnected frameworks of materials that contain void spaces or pores. Due to their unique topology and depending on the base material, porous materials possess special characteristics that make them suitable to be used for many purposes. The most significant property of these materials is their multifunctional lightweight structure, which in combination with their other properties like high specific strength and structural rigidity, thermal and acoustic insulation, energy absorption capacity and

N. Ghiasi (✉) · S. Diebels (✉)
Applied Mechanics, Saarland University, Campus A4 2, Saarbrücken 66123, Saarland, Germany
E-mail: narges.ghiasi70@gmail.com

S. Diebels (✉)
E-mail: s.diebels@mx.uni-saarland.de

P. Sharma (✉) · A. Jung (✉)
Protective Systems, Helmut-Schmidt University/ University of the Federal Armed Forces Hamburg, Holstenhofweg 85, Hamburg 22043, Hamburg, Germany
E-mail: sharmap@hsu-hh.de

A. Jung (✉)
E-mail: junga@hsu-hh.de

vibrational damping make them an interesting material in many fields of engineering like aerospace and automotive industries, biomedical implants and construction applications [1]. Furthermore, permeability and large internal surface area, especially in open-cell foams, make these materials perfect candidates to be used as filters, heat exchangers, electrodes, batteries and bearings [2,3].

Common materials used to manufacture solid porous materials are metals, polymers and ceramics. However, polymer foams are the most commercialized variety [4]. Polymer foams offers many advantages: low relative density, excellent performance of heat and sound insulation, and good energy absorption. However, it is difficult for them to fulfil conditions where high strength, high energy absorption capacity and high temperature tolerance are needed simultaneously. Porous metals, on the other hand, not only have the typical characteristics of metals like weldability and electrical conductivity, but also can meet the above-mentioned characteristics [3]. However, problems such as their expensive manufacturing process and bad reproducibility may result in the limited application of metal foams [5]. The increasing applications of porous metals over the past years led to the improvement of their different production procedures. Many innovations were proposed in this field. Hybrid metal foams are one of the suggested solutions that could partially compensate the mentioned shortcomings. Hybrid metal foams are basically open-cell foams that are coated by a metallic layer via an electrodeposition process [6,7]. The major advantages of this method are twofold: First, the properties of the foam can be improved based on the mechanical properties of the chosen coating material and by tailoring the coating thickness. Second, based on the material of the template, the manufacturing costs can be significantly reduced [8]. One of the recent types of hybrid foams is the polyurethane foam that is coated with nanocrystalline nickel which is briefly referred to as Ni/PU hybrid foam. The main advantages of these hybrid foams are that they possess the lightweight characteristics of highly porous solids and the strength of nickel while being economical in comparison with similar metal foams. Jung and Diebels [8] showed that Al and PU hybrid foams coated with nickel have similar mechanical properties, but Ni/Al is more expensive by an order of magnitude.

One of the methods to produce Ni/PU foams is the electrodeposition method. It is a conventional process that uses an electric current to form a thin layer of metal coating on the surface of a conductive material. In this process, positively charged desired metal ions (cations) which are dissolved in the electrolyte are deposited on the surface of the substrate connected to the negatively charged electrode (cathode) by the passage of electric current. Electrodeposition has been a subject of interest to metallurgists due to its capability in producing new materials with modified properties in any arbitrary three-dimensional geometries. Jung et al. [8,9] were among the first who used an electrodeposition process to produce Ni/PU hybrid foams and compared the advantages of this method with conventional production methods like chemical vapour deposition (CVD) or electroless plating. However, there are some hindrances when it comes to the coating of porous structures and especially of porous polymers. One of these problems is the heterogeneous coating thickness due to mass transport limitations [10–12] which results in a heterogeneous distribution of the mechanical properties in the hybrid foam. Up to now, the optimization of the electrodeposition process is performed based on a trial-and-error approach. Since the focus of this study is on Ni/PU foams and the modelling of the coating process, in the following the electrodeposition process for these hybrid foams is described briefly.

1.1 Pretreatment of polyurethane foams

For the electrodeposition process, it is required for the substrate to be electrically conductive so that it can be coated by an electrodeposition process. However, polyurethane is a non-conductive polymer that needs a special pretreatment procedure. So, the first step is to make PU foams electrically conductive by dip coating the open-cell foams in a conductive graphite lacquer. To remove the excess lacquer from the pores and struts, a compressed airflow is blown through the foams [9,13]. The dip-coated foam is used as a template for the Ni/PU foam in the electrodeposition process.

1.2 Electrodeposition process

The aqueous nickel sulphamate electrolyte contains Ni^{2+} ions as nickel source for the coating process. In the beginning, under the absence of an electrical current, the porous template is plunged into the aqueous electrolyte with homogeneously distributed nickel ions and connected to the cathode. It is assumed that the electrolyte is supplied with an infinite nickel ion source with the concentration C_∞, realized by two sacrificial

anodes on both sides of the foam [14]. Under an applied external electrical field, positively charged nickel ions (cations) migrate to the polyurethane substrate (cathode), where they are discharged and deposited as metallic nickel layer according to

$$Ni^{2+} + 2e^{-} \rightarrow Ni \tag{1}$$

This leads to a decreasing ion concentration in the pores of the foam. The resulting inhomogeneity in concentration is reduced by diffusion of ions in the electrolyte. A pump can also be used to drive the flow and to distribute the ions in the foam more homogeneously, when pure diffusion is too slow due to low concentration gradient [9,14].

As a result of the reaction, two zones with different ion concentration will be developed in the electrolyte: one far away from the cathode (substrate) with constant concentration C_∞ and the other zone in the vicinity of the cathode with lower concentration. Hence, the mass transport is required to compensate the decrease in the ion concentration close to the substrate and driven by the deposition process. The mass transport is mainly governed by three processes: migration, which is the motion of ions due to the electrical potential gradient, convection, which is the motion of ions due to the pump pressure, and diffusion, which is the motion of ions due to the concentration gradient in the electrolyte. Moreover, nickel ions react with the electrons on the foam cathode, forming a metallic coating layer, and hence introduces a sink term for the ions in the electrolyte which is the responsible term for the coating process [13].

In spite of many advantages, this coating process is also accompanied with a lot of shortcomings and problems such as mass transport limitation which finally leads to a heterogeneous distribution of the coating thickness on the porous foam [9,14]. Therefore, it is important to reach a numerical model which can describe the process precisely. The goal is to use the model to identify the optimized process parameters and improve the experiment in order to achieve a homogeneous distribution of the coating thickness which results in homogeneous mechanical properties. Hughes et al. [15] developed the equations for modelling electrodeposition under forced convection and used numerical algorithms to set up a simulation. Joekar-Niasar et al. [16] investigated the coupled hydrodynamic and electrochemical interactions caused by the presence of charged solid surfaces, ions in the fluid and chemical reactions between the ions in the fluid and the solid surface. However, there are only few studies on the simulation of coating of complex structures like porous materials. Grill et al. [17,18] numerically simulated the electroplating process of open-cell foams and investigated the influence of electrodeposition parameters. In another study, Grill et al. [13] simulated the electrodeposition process of nickel ions on polyurethane foams and investigated the homogeneity of the coating thickness and, finally, compared the numerical results with the experimental data. The model that was developed by Grill et al. is based on the Nernst–Planck equation, where they deal with a one-sided coupled electrodeposition process. In their model, they assume constant values for process parameters such as velocity and electrical field as well as geometrical parameters such as porosity and permeability. However, in the real process all the parameters change due to geometrical changes caused by the coating.

The objective of this study is to mathematically model the above-mentioned process on a macroscopic scale. This article is based on and part of the doctoral thesis, "Numerical modelling of Ni/PU hybrid foams coating process" [19]. The presented model in this study is based on the mixture theory where a system of governing equations is derived from balance equations and suitable constitutive equations. It is a two-sided coupled simulation in which the influence of coating on all the other parameters such as porosity and permeability is investigated. To accomplish this, the process and the geometrical properties are assumed as simple as possible to reduce the number of process parameters. The changes in the flux velocity will be taken into account by calculation of pressure from an additional Darcy equation. Moreover, the evolution of the electrical field will be studied by coupling a third equation to the system of equations. In the next section, the governing equations describing the process are developed using mixture theory along with simplifying assumptions. To validate the model, in Sect. 3, the equations are implemented for a simple 1D domain where the changes in variables are only considered in the flow direction. The finite difference scheme has been used to solve the equation system. Finally, Sect. 4 provides the obtained conclusions and a summary of the study, as well as possible future extensions.

2 Mathematical model

In this section, a mathematical model for the electrodeposition process of nickel ions on polyurethane foams is proposed. Due to complexities arisen by the multi-scale characteristic of the problem, it is necessary to simplify

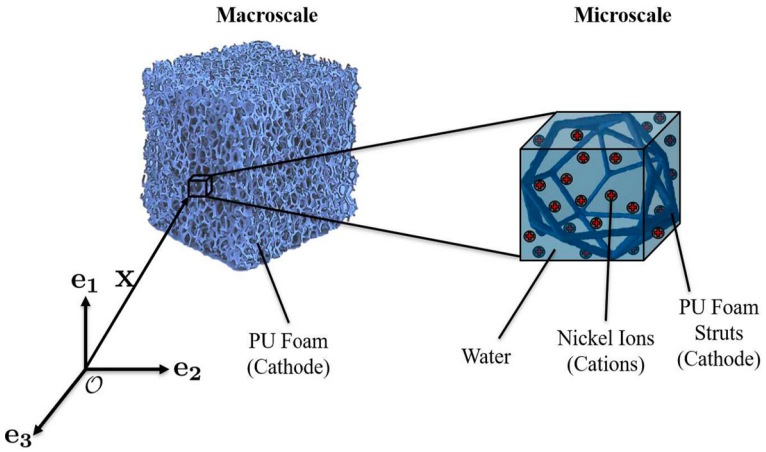

Fig. 1 Schematic representation of problem as a three-phase mixture. A material point on the macroscale can be resolved on the microscale by an REV

the model as much as possible and only consider the essential features in the macroscale without going into exact microscale mechanical and geometrical details. Therefore, mixture theory gives an appropriate framework for the development of such a model [19].

Modelling the flow behaviour through a porous medium requires a formulation in the framework of multi-phase continuum mechanics. In these types of problems, the representative elementary volume (REV) under study is no longer a single continuous material, but it rather consists of two or more constituents which simultaneously occupy the same macroscopic position, leading to the concept of superimposed continua. On that account, the problem is investigated in the framework of mixture theory and theory of porous media (TPM) [20,21], as shown in Fig. 1.

In this figure, the spatial position $\mathbf{x}$ in the mixture is occupied simultaneously by three constituents. The domain in the current configuration is occupied by a solid phase, φ^{s}, which is in fact the porous skeleton, and a fluid phase, φ^{f}, which fills the pores. The fluid phase, i.e. the electrolyte, itself is assumed to be a two-component phase, namely water, φ^{w}, and nickel ions, φ^{ni}. For the sake of simplicity, the other constituents in the fluid phase are neglected.

Different properties can be defined for each constituent occupying the same spatial point on the macroscale. Following the concepts of mixture theory, e.g. Trussdell [22], Bowen [20], etc., the first step is to specify the kinematics and field equations.

The partial density (kg/m^3) of each constituent φ^i, i={s, w, ni} can be defined as the ratio of the mass of the constituent, dm^i, to the total volume of REV, dV,

$$\rho^i = \rho^i(\mathbf{x}, t) = dm^i/dV = (dV^i/dV)\rho^{iR}(\mathbf{x}, t) \tag{2}$$

where ρ^{iR} is the real or intrinsic density of each constituent and dV^i is the occupied volume by constituent i. The term (dV^i/dV) represents the volume fraction of each constituent i.

Therefore, the total mixture density at each spatial point is the summation of the partial densities of all n constituents at that point

$$\rho = \rho(\mathbf{x}, t) = \sum_{i=1}^{n} \rho^i(\mathbf{x}, t) \tag{3}$$

Moreover, the mass concentration of each constituent φ^i at the spatial position $\mathbf{x}$ is defined as

$$c^i = c^i(\mathbf{x}, t) = \rho^i/\rho \tag{4}$$

Different velocities can be defined for the mixture as a whole and for each constituent. The mixture mean or barycentric velocity $\mathbf{v}$ at $(\mathbf{x}, t)$ is the velocity of its centre of mass which is defined by

$$\mathbf{v}(\mathbf{x}, t) = \frac{1}{\rho}\sum_{i=1}^{n} \rho^i \mathbf{v}^i(\mathbf{x}, t) = \sum_{i=1}^{n} c^i \mathbf{v}^i(\mathbf{x}, t) \tag{5}$$

where $\mathbf{v}^i$ is the velocity of each constituent (m/s).

Another velocity defined in mixture theory is the *diffusion velocity* $\mathbf{u}^i$, which is the relative velocity of constituent i with respect to the centre of mass of the mixture and is formulated as

$$\mathbf{u}^i(\mathbf{x}, t) = \mathbf{v}^i(\mathbf{x}, t) - \mathbf{v}(\mathbf{x}, t) \tag{6}$$

According to Trussdell's metaphysical principles, the balance equations of individual constituents are identical to the balance equations of a single-phase continuum except for the local interactions of the constituents. These interactions are taken into account by appropriate production terms. During the deposition process, the nickel ions are decreasing and the solid mass is increasing. However, the water constituent does not take part in the mass exchange process. Therefore, the balance equations of mass for each constituent at point $\mathbf{x}$ can be written as

$$\text{Solid:} \quad \frac{\partial \rho^{\mathrm{s}}}{\partial t} + \operatorname{div}(\rho^{\mathrm{s}}\mathbf{v}^{\mathrm{s}}) = \hat{\rho}^{\mathrm{s}} \tag{7}$$

$$\text{Water:} \quad \frac{\partial \rho^{\mathrm{w}}}{\partial t} + \operatorname{div}(\rho^{\mathrm{w}}\mathbf{v}^{\mathrm{w}}) = 0 \tag{8}$$

$$\text{Nickel ions:} \quad \frac{\partial \rho^{\mathrm{ni}}}{\partial t} + \operatorname{div}(\rho^{\mathrm{ni}}\mathbf{v}^{\mathrm{ni}}) = \hat{\rho}^{\mathrm{ni}} \tag{9}$$

Using Eq. (3), the balance equation of mass for the mixture as a whole can be obtained by summation of mass balances of all constituents (Eqs. (7), (8) and (9)). Moreover, according to the mass conservation principle, the total mass of the system remains constant and there will be no total mass production. Hence, the right-hand side of the equation should be equal to zero.

$$\text{Mixture:} \quad \frac{\partial \rho}{\partial t} + \operatorname{div}(\rho\mathbf{v}) = \hat{\rho}^{\mathrm{s}} + \hat{\rho}^{\mathrm{ni}} = 0 \tag{10}$$

In these equations, $\frac{\partial}{\partial t}$ is the partial derivative with respect to the time and div(•) is divergence with respect to the Eulerian system, related to the gradient operator defined as

$$\operatorname{grad}(\bullet) = \frac{\partial(\bullet)}{\partial \mathbf{x}} \tag{11}$$

The quantity $\hat{\rho}^i$ is called the *mass production* (kg/m^{3}s) of constituent φ^i, i={s, ni} and it represents the rate of mass supplied to the ith constituent from the other constituents in the same spatial position. Since the mass of the mixture should remain unchanged, the total amount of mass production in the mixture is equal to zero, according to Eq. (10). Therefore,

$$\hat{\rho}^{\mathrm{s}} = -\hat{\rho}^{\mathrm{ni}} \tag{12}$$

That means that the deducted amount of nickel ions from the electrolyte is deposited on the solid and will further contribute to the solid's mass.

The mass balance equation for the fluid phase (water + nickel) is obtained by summing Eqs. (8) and (9).

$$\frac{\partial \rho^{\mathrm{f}}}{\partial t} + \operatorname{div}(\rho^{\mathrm{f}}\mathbf{v}^{\mathrm{f}}) = \hat{\rho}^{\mathrm{ni}} \tag{13}$$

The solid phase is assumed to be rigid and stationary without any deformation. Moreover, it has no motion and hence no velocity. Therefore, it would be simpler if only the pore fluid (water + nickel) is considered instead of the whole three-phase mixture (solid + water + nickel), and the effect of solid on the fluid is considered only through forces.

In a simplified setting, the process can be described by defining appropriate constitutive equations for the flux. It consists of a diffusion and migration part which can be described by Fick's law and a pressure driven (convective) part that is described by a generalized Darcy's law. In the next subsection, the governing equations will be derived using the suitable constitutive equations.

2.1 Derivation of governing equations

In order to establish a model which accounts for the coating thickness, it is necessary to derive the equations that determine the distribution of concentration rate within the porous medium. Furthermore, due to the velocity changes, as a result of changes in geometry within the foam, developing a pressure formulation is of importance, since the concentration rate is coupled with pressure rate. The simplified model consists of mass balances of fluid and nickel phases and constitutive assumptions for the mass fluxes, instead of additional momentum balances and constitutive models for partial stresses and momentum exchange.

During the deposition process, the primary ions involved in the increase of the solid mass are the positive nickel ions (c^+). Nickel is dissolved to positively charged nickel ions and electrons (Eq. (1)). This happens mainly close to the cathode. The flux of electrons is in equilibrium with the external applied current while only the nickel ions travel to the foam (anode) and are deposited and reduced to elementary nickel. Therefore, in this study only the concentration of the positive ions is needed.

Considering the fluid phase as the REV, based on Eq. (4) the mass concentration of nickel ions can be defined as

$$c^{\mathrm{ni}} = \frac{\rho^{\mathrm{ni}}}{\rho^{\mathrm{f}}} \tag{14}$$

The fluid barycentric velocity $\mathbf{v}^f$ at $(\mathbf{x}, t)$, according to Eq. (5), is defined by

$$\mathbf{v}^{\mathrm{f}}(\mathbf{x}, t) = \frac{1}{\rho^{\mathrm{f}}} \sum_{i=\{\mathrm{w},\ \mathrm{ni}\}} \rho^i \mathbf{v}^i(\mathbf{x}, t) = \sum_{i=\{\mathrm{w},\ \mathrm{ni}\}} c^i \mathbf{v}^i(\mathbf{x}, t) \tag{15}$$

where $\mathbf{v}^i$ is the velocity of each constituent in the fluid phase. Hence, Eq. (6) results in

$$\mathbf{v}^{\mathrm{ni}} = \mathbf{v}^{\mathrm{f}} + \mathbf{u}^{\mathrm{ni}} \tag{16}$$

In this study, the main variable of interest is the concentration of nickel ions. So, for simplicity in the rest of this article it is illustrated by c instead of c^{ni}.

To investigate the flow behaviour through the porous medium, a linear relation between the velocity and the pressure gradient of flow can be derived as a special case of the fluid momentum balance [21,23].

$$\rho^{\mathrm{f}} \frac{\partial \mathbf{v}^{\mathrm{f}}}{\partial t} + \rho^{\mathrm{f}} \mathrm{grad}\mathbf{v}^{\mathrm{f}} \cdot \mathbf{v}^{\mathrm{f}} = \mathrm{div}\boldsymbol{\sigma}^{\mathrm{f}} + \rho^{\mathrm{f}}\mathbf{g} + \hat{\mathbf{p}}^{\mathrm{f}} \tag{17}$$

In this equation, $\boldsymbol{\sigma}^f$ is the partial stress tensor (Pa), $\mathbf{g}$ is the external body force (e.g. gravity) (m/s^2) and $\hat{\mathbf{p}}^f$ is called the momentum production (kg/m^2 s^2) which accounts for the change of momentum of a phase due to stresses imposed on it by the other phases.

The forces acting on the mixture are assumed to be composed of a hydrostatic pressure, which exerts a compressing normal stress, and a part which produces shear stresses. The fluid momentum production $\hat{\mathbf{p}}^f$ contains forces such as buoyancy which is related to average pressure and gradient of volume fraction, and a viscous drag which can be correlated to volume fractions and average velocity differences. Also, the fluid mixture is assumed to have a low viscosity, which minimizes the impact of viscous stresses on the overall flow dynamics. Neglecting the viscous forces in the formulation of stress and including the viscosity effects in the momentum interaction term, the stress tensor applied on the fluid phase and the momentum production can be defined as follows, respectively:

$$\boldsymbol{\sigma}^{\mathrm{f}} = -n^{\mathrm{f}} p \mathbf{I} \tag{18}$$

$$\hat{\mathbf{p}}^{\mathrm{f}} = (n^{\mathrm{f}})^2 K(\mathbf{v}^{\mathrm{s}} - \mathbf{v}^{\mathrm{f}}) + p\ \mathrm{grad}\, n^{\mathrm{f}} \tag{19}$$

In these equations, n^{f} is the volume fraction of the fluid part which is equivalent to the volume fraction of pore space, or simply porosity, and K is the *drag coefficient* (kg/m^3 s) due to relative motion and is defined as the ratio of viscosity of flow to the intrinsic permeability of the porous medium [23,24].

$$K = \frac{\mu}{k} \tag{20}$$

It is assumed that the fluid is a Newtonian fluid with laminar flow through a rigid porous solid. Due to the assumption of small Reynolds number for the flow, the fluid inertia can be neglected, compared to the interaction forces of the fluid and the solid matrix. To simplify the problem and based on the small magnitudes of the electrical field, the terms in the momentum equation describing the electrical forces due to the charged ions are considered negligible and the effect of the electric field is considered in the diffusion velocity, which depicts the deformation due to electrical forces through a migration term. Also, the flow is assumed to be stationary, and hence, there is no acceleration. That means the material time derivative of fluid velocity is equal to zero. Therefore, by substituting Eqs. (18) and (19) into the Eq. (17) and applying the above-mentioned assumptions, it is concluded that:

$$0 = \operatorname{div}(-n^{\mathrm{f}} p\mathbf{I}) + \rho^{\mathrm{f}}\mathbf{g} + (n^{\mathrm{f}})^2 K(-\mathbf{v}^{\mathrm{f}}) + p \operatorname{grad} n^{\mathrm{f}} \tag{21}$$

Therefore, the fluid mean barycentric velocity can be expressed in terms of pressure gradient as:

$$\mathbf{v}^{\mathrm{f}} = \frac{-1}{n^{\mathrm{f}} K}(\operatorname{grad} p - \rho^{\mathrm{fR}}\mathbf{g}) \tag{22}$$

By substituting Eq. (22) into the mass balance Eq. (13) of the fluid, and Eqs. (14) and (16) into the mass balance Eq. (9) of the nickel ions, it is concluded that

$$\frac{\partial \rho^{\mathrm{f}}}{\partial t} + \operatorname{div}\left(\frac{-\rho^{\mathrm{f}}}{n^{\mathrm{f}} K}\left(\operatorname{grad} p - \rho^{\mathrm{fR}}\mathbf{g}\right)\right) = \hat{\rho}^{\mathrm{ni}} \tag{23}$$

$$\rho^{\mathrm{f}}\frac{\partial c}{\partial t} + \frac{-\rho^{\mathrm{f}}}{n^{\mathrm{f}} K}\left(\operatorname{grad} p - \rho^{\mathrm{fR}}\mathbf{g}\right) \cdot \operatorname{grad} c = (1-c)\hat{\rho}^{\mathrm{ni}} - \operatorname{div}\left(\rho^{\mathrm{ni}}\mathbf{u}^{\mathrm{ni}}\right) \tag{24}$$

Taking a glance at Eqs. (23) and (24), it can be seen that they are in terms of the primary unknowns which are pressure p and concentration c. However, there are still three more unknowns, namely partial density of fluid ρ^{f}, the production term $\hat{\rho}^{\mathrm{ni}}$ and the diffusion velocity of ions $\mathbf{u}^{\mathrm{ni}}$. That arises the need for defining three more constitutive equations in terms of the primary unknowns to reach to a closed system of equations.

The diffusive flux $\rho^{\mathrm{ni}}\mathbf{u}^{\mathrm{ni}}$, relative to the motion of the fluid phase, is partly due to the concentration gradient of ions in the electrolyte which introduces a diffusion term, and partly caused by the electrical field which results in a migration term. The effect of tortuosity in open-cell foams are negligible. Hence, the mass transfer can be described by Fick's law [20] for the dispersive flux, which alongside the migration term will result in the whole flux term as

$$\rho^{\mathrm{ni}}\mathbf{u}^{\mathrm{ni}} = -\mathbf{D} \cdot \operatorname{grad} c - \frac{zF}{R\theta} Dc \operatorname{grad} \phi \tag{25}$$

In Eq. (25), $\mathbf{D}$ is the dispersion tensor (kg/m s), z is the electric charge of the ions, F is the Faraday constant (C/mol), R is the universal gas constant (Nm/ K mol), θ is the absolute temperature (K) and ϕ is the electrical potential (V). For the sake of simplicity, the dispersion tensor is assumed to be equal to the mixture diffusivity constant D times the identity matrix.

The next step is to define a relation for the production term. Evidently, the larger the ion concentration is, the larger the production term will be. Hence, the constitutive equation for the production term can be defined in the simplest case as

$$\hat{\rho}^{\mathrm{ni}} = A_1 c \tag{26}$$

The parameter A_1 may additionally depend on further local and macroscopic quantities, e.g. the electrochemical potential. It represents the rate of mass production of nickel ions, which is influenced by different factors such as local ion concentration and electrochemical potential. Here, for the sake of simplicity, it will be assumed to be a constant. However, it can vary based on the local conditions.

The last equation is concerning the fluid density which can be defined as an equation of state of a barotropic fluid. There is a direct relation between fluid density, pressure and ion concentration. So we can define an equation based on the first terms in a Taylor series expansion of $\rho^{\mathrm{f}}(c, p)$

$$\rho^{\mathrm{f}} = \rho_0 + A_2 c + A_3(p - p_0) \tag{27}$$

where ρ_0 is the density of pure water and p_0 is the reference pressure. However, the fluid is assumed to be incompressible. Therefore, the pressure changes should not have a profound influence and its effect should be way smaller than the effect of the concentration, resulting in $A_3 \ll A_2$.

The parameters A_1, A_2 and A_3 in Eqs. (26) and (27) are unknown constants that must be identified through parameter identification.

Finally by substituting Eqs. (25)–(27) into Eqs. (23) and (24), the final coupled governing equation system can be obtained.

$$\begin{aligned}\frac{\partial c}{\partial t} &= \frac{1}{\rho_0 + A_2 c + A_3(p - p_0)}\Big[A_1 c(1-c) + D\,\mathrm{div}(\mathrm{grad}c) \\ &\quad + \frac{zFD}{R\theta}(\mathrm{grad}c \cdot \mathrm{grad}\phi + c\ \mathrm{div}(\mathrm{grad}\phi))\Big] \\ &\quad + \frac{1}{n^{\mathrm{f}}K}\left(\mathrm{grad}p - \rho^{\mathrm{fR}}\mathbf{g}\right)\cdot \mathrm{grad}c \qquad (28)\\ \frac{\partial p}{\partial t} &= \frac{1}{A_3}\Big[(A_1 c)\left(1 - \frac{A_2}{\rho_0 + A_2 c + A_3(p-p_0)}(1-c)\right) \\ &\quad - \frac{A_2 D}{\rho_0 + A_2 c + A_3(p-p_0)}\Big[\mathrm{div}(\mathrm{grad}c) + \frac{zF}{R\theta}(\mathrm{grad}c\cdot\mathrm{grad}\phi + c\ \mathrm{div}(\mathrm{grad}\phi))\Big] \\ &\quad + \frac{\rho_0 + A_2 c + A_3(p-p_0)}{n^{\mathrm{f}}K}\big[\mathrm{div}(\mathrm{grad}p)\big] + \frac{A_3}{n^{\mathrm{f}}K}((\mathrm{grad}p)^2 - \rho^{\mathrm{fR}}\mathbf{g}\cdot\mathrm{grad}p)\Big] \qquad (29)\end{aligned}$$

Taking a glance at Eqs. (28) and (29), one can clearly observe the contribution of different ionic transport mechanisms (diffusion, convection, migration and sink term) to the whole electrodeposition process. However, it is still necessary to describe the electrical potential, ϕ, through the electric field, $\mathbf{E}$, formed by the applied external current and movement of ions. The electric field is related to the electrical potential as

$$\mathbf{E} = -\mathrm{grad}\phi \qquad (30)$$

The displacement current equation describes the temporal change of the electric field according to the following equation [25,26]:

$$\frac{\partial \mathbf{E}}{\partial t} = \frac{\mathbf{I}_{ext}}{\epsilon} - \frac{Fz\mathbf{J}}{\epsilon} \qquad (31)$$

where $\mathbf{I}_{ext}$ is the external current density (A/m^2), ϵ is the absolute permittivity (C^2/N m^2) and $\mathbf{J}$ is the flux of ions (mol/m^2 s) due to different mass transfer mechanisms. This can be described inspired by Eq. (25) and additional convective term. Since the solid phase does not contribute to the ionic transport, the overall average flux through the REV is related to the fluid phase.

$$\mathbf{J} = c^*\mathbf{v} - D\ \mathrm{grad}c^* - \frac{zF}{R\theta}Dc^*\ \mathrm{grad}\phi \qquad (32)$$

The term c^* in Eq. (32) is the ion concentration and has the unit mol/m^3. In order to make this compatible to the definition for ion concentration in this article, c^* is replaced by the following relation in terms of c

$$c^* = \frac{c\rho^{\mathrm{f}}}{MW^{\mathrm{ni}}} \qquad (33)$$

where MW^{ni} is the molar weight of nickel (kg/mol).

By substituting Eqs. (30) and (32) into Eq. (31), it is possible to calculate the rate of gradient of electric potential. This equation alongside with Eqs. (28) and (29) yields a coupled system of equations that should be solved simultaneously. With the help of this system of equations, the time derivative of concentration and pressure within the foam can be calculated. In the considered simplified model, these data can be used to estimate the distribution of ions on the foam and finally to give an estimation of the coating thickness.

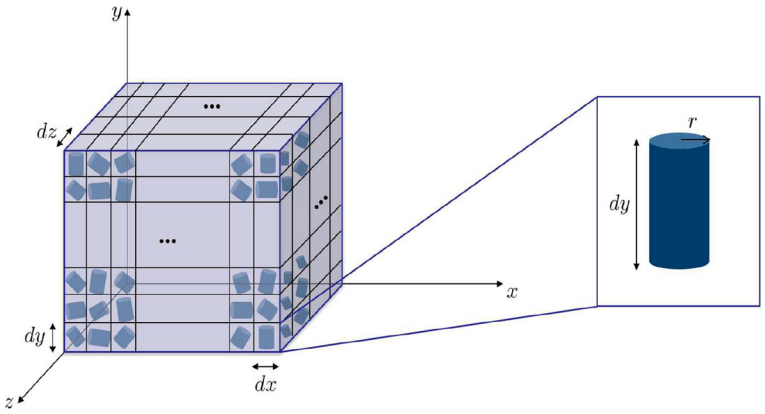

Fig. 2 Schematic representation of struts inside each volume element

2.2 Back-coupling formulation

In the previous subsection, the equations to calculate the concentration and pressure rate are obtained from the balance equations of mass. However, it is important to consider the changes within the foam structure during the coating process, which lead to a change in all the other parameters.

The aim in the present study is to assume the process as simple as possible so that the number of process parameters can be reduced. Therefore, the description of the geometrical properties have to be as simple as possible. In this idealization, the struts are considered as simple cylinders and the nodes between the struts are disregarded.

The concentration obtained from Eq. (28) gives the information about the transported nickel ions by diffusion, convection and migration mechanisms as well as the deducted nickel ions from the fluid phase which are coated on the foam struts. Using this concentration data, it is possible to estimate the coating thickness in each spatial point on the foam.

Moreover, with the start of the coating process, the porosity of the foam will start to change, which results in a change in permeability.

Hence, a back-coupling is necessary in order to take into account the above-mentioned geometrical changes and to use the updated values to calculate the variables in the next time steps. As shown in Fig. 2, the foam is divided into small volume elements. It is assumed that these volume elements are so small that inside each of them only one strut can fit. The struts can be represented by cylindrical figures. Therefore, with nickel deposition inside each volume element, the radius of these cylinders will increase.

To simplify the problem, it is assumed that all the struts inside each volume element have the same size at the beginning of the coating process. Moreover, it is assumed that the initial total porosity is equal to the initial porosity of each volume element. The total volume of each volume element, dV^{el}, can be obtained as

$$dV^{\mathrm{el}} = dxdydz \tag{34}$$

The volume, dv^{s}, and surface, ds^{s}, of each strut inside each volume element are

$$dv^{\mathrm{s}} = \pi r^2(\mathbf{x}, t)dy \tag{35}$$

$$ds^{\mathrm{s}} = 2\pi r(\mathbf{x}, t)dy \tag{36}$$

The term dy is related to the volume element size which can be assumed to be the same as the spatial grid size in FDM formulation.

Hence, according to the theory of porous media, the initial radius of the struts can be calculated from the solidity,

$$n^{\mathrm{s}} = 1 - n^{\mathrm{f}}, \tag{37}$$

as

$$n^{\mathrm{s}}(\mathbf{x}, 1) = \frac{dv^{\mathrm{s}}(\mathbf{x}, 1)}{dV^{\mathrm{el}}} \tag{38}$$

With the start of the process, the nickel ions are coated on the surface of the strut inside the volume element. The rate of change of the coating thickness will be equivalent to the radius change

$$\Delta r(\mathbf{x}, t) = \frac{\hat{V}(\mathbf{x}, t)}{ds^{\mathrm{s}}(\mathbf{x}, t)} \tag{39}$$

The term $\hat{V}(\mathbf{x}, t)$ in Eq. (39) is the volume of the coating and is proportional to the production term.

$$\hat{V}(\mathbf{x}, t) \propto \hat{\rho}^{\mathrm{ni}}(\mathbf{x}, t) \tag{40}$$

Therefore, by calculating the new volume and surface of the strut, the new radius, the new solidity and therefore the new porosity can be calculated. The proportionality constant in Eq. (40) can be defined in terms of nickel density ρ_0^{ni}, as

$$\hat{V}(\mathbf{x}, t) = \hat{\rho}^{\mathrm{ni}}(\mathbf{x}, t)\ \frac{V^{\mathrm{el}}}{\rho_0^{\mathrm{ni}}}\, dt \tag{41}$$

This equation will give the volume of deposited nickel in each volume element in each time step. Hence, the mean local coating thickness at each point, $\delta(\mathbf{x})$, can be calculated as

$$\delta(\mathbf{x}) = \int \Delta r(\mathbf{x}, t)\, \mathrm{d}t \tag{42}$$

Many practical equations are suggested in the literature for porosity–permeability relation, which have been discussed comprehensively in a review article by Hommel et al. [27]. Using these equations, e.g. exponential or power law relations, the new permeability can be obtained. The following relation has been chosen from [27] to calculate the new permeability

$$\frac{K}{K_0} = \left(\frac{n^{\mathrm{f}}}{n_0^{\mathrm{f}}}\right)^{\eta} \tag{43}$$

The exponent η in this equation is an empirical parameter [27], which depends on the local topology of the foam and has to be determined from experiments.

Hence, based on these updated values of porosity and permeability, the pressure and concentration in the next time step will be calculated.

2.3 Numerical formulation

In the present study, a finite difference method (FDM) [28–31] is employed to solve the preceding coupled equations with defined initial and boundary conditions. The finite difference method is an easy and direct numerical approach to solve nonlinear partial differential equations (PDE), which is a suitable choice for the purpose of this study.

An explicit approach is used to discretize these time- and space-dependent PDEs. FDM offers different discretization schemes for different problems. In this study, a forward scheme is used for the time derivatives and a central scheme is used for second-order spatial derivatives resulting from diffusive processes. Since the convection term in Eq. (28) consists of a term specifying the direction of flow, an upwind discretization scheme is of interest here. This argument is also applicable to the migration terms in both equations because the mathematical structure of the migration term is the same as in the convective part.

The resulting scheme is simple and does not require to solve a coupled set of equations. As a disadvantage though, the scheme is of limited stability. Based on stability analyses, e.g. by von Neumann [28–31], backward scheme results in more stable answers for the convection term in Eq. (29).

In the following section, a problem with corresponding initial and boundary conditions will be defined and the validity of this model will be evaluated.

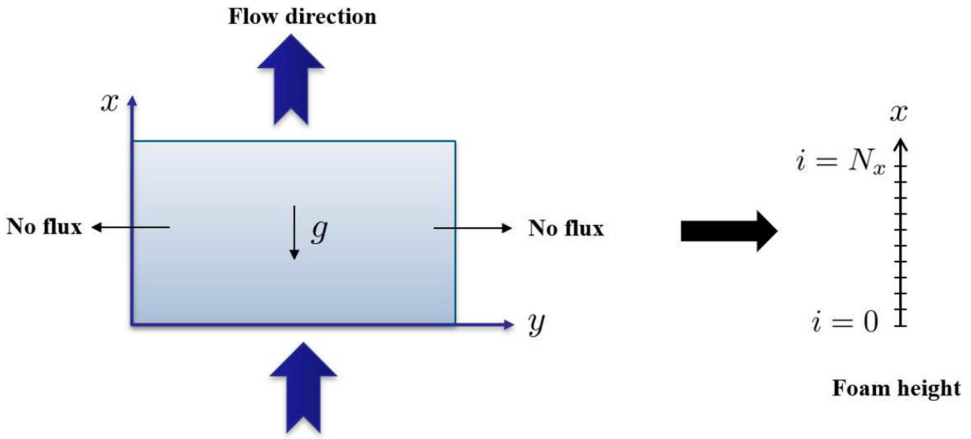

Fig. 3 Problem domain with the direction of flow against the gravity

3 Results and discussions

In this section, a hypothetical problem will be defined to investigate the performance of the proposed model [19]. For the sake of simplicity and an efficient interpretation of results, normalized values are defined for time and space domain and the primary variables (pressure and concentration) are investigated in terms of normalized values. Normalization is obtained by the maximum magnitudes of concentration and pressure at the inlet of the reaction cell. Therefore, the model is validated on a computational domain with a length of 1, as shown in Fig. 3. Moreover, the electric field due to the movement of ions is neglected and it is assumed that it is only formed by the applied external current. For the sake of simplicity, it is assumed that the parameters are changing only in the flow direction while they are constant in other directions. Therefore, it is possible to consider the problem as a one-dimensional problem. Based on the 1D assumption, the problem is only solved in flow direction in the mid-plane of the specimen.

A general overview of the experiment has been given in section 1. The initial and boundary conditions are defined corresponding to the experiment's conditions [9]. At the beginning of the process, the pump is off and also no electrical current is applied on the system. Keeping this in mind alongside with the assumption of an infinite ion reservoir, the initial conditions are as follows:

$$c(x, 0) = C_\infty \tag{44}$$

$$p(x, 0) = p_0 \tag{45}$$

$$E(x, 0) = E_0 \tag{46}$$

When the pump is turned on, it takes a time t_1 for it to reach to the designated pressure p_{max} at the inlet. Moreover, the applied external electric current alongside with the infinite ion reservoir results in the following boundary conditions at the inlet of the foam:

$$c(0, t) = C_\infty \tag{47}$$

$$p(0, t) = \begin{cases} \dfrac{p_{max}\ t}{t_1} & t \le t_1 \\ p_{max} & t > t_1 \end{cases} \tag{48}$$

$$E(0, t) = E_1 \tag{49}$$

On the outlet of the foam, a Neumann type boundary condition will be defined for concentration, reflecting the strong influence of convection. Moreover, the pressure reaches the constant outlet pressure p_0. Hence, the boundary conditions at the outlet are:

$$\left.\frac{\partial c(x, t)}{\partial x}\right|_{x=1} = 0 \tag{50}$$

$$p(1, t) = p_0 \tag{51}$$

$$E(1, t) = E_1 \tag{52}$$

Table 1 Magnitudes of problem's physical constants

Constant	Value	Constant	Value
ρ_0	1000 kg/m^3	D	6.8×10^{-10} kg/m s
z	2	F	96485.33 C/mol
R	8.31 Nm/Kmol	θ	323 K
ϵ	70 C^2/Nm^2	I_{ext}	16.5 A/m^2
K	1.3×10^5 kg/m^3 s	n^{f}	0.9
g	9.8 m/s^2	η	8

Table 2 Assumed magnitudes of input variables

Constant	Value	Constant	Value
A_1	-1×10^2	A_2	1.5×10^3
A_3	2×10^{-1}	dx	1×10^{-2}

It is assumed that the process is performed under constant temperature of 50° C, with an external current density of 16.5 A/m^2 and on a PU foam with 90 per cent porosity [9]. The magnitudes of different physical constants in Eqs. (28), (29) and (31) are listed in Table 1.

The diffusion coefficient D is assumed to be equal to the ionic diffusion coefficient of Ni^{2+} in free water [32]. Moreover, the exponent η is an empirical parameter and chosen based on the data found in [27].

For the back-coupling calculations, the volume elements are assumed to be cubes with edge length dx. Hence, the input variables in the problem are chosen as listed in Table 2.

According to Eq. (27) and the incompressibility assumption, the effect of pressure change on the electrolyte density is negligible compared to the concentration change. Hence, the pressure constant A_3 must be much smaller than the concentration constant A_2. Also A_1 is a sink constant and therefore must be negative.

The representative normalized time and space ranges and steps are defined as:

$$0 \leq t \leq 1; \quad \Delta t = 10^{-3} \tag{53}$$

$$0 \leq x \leq 1; \quad \Delta x = 10^{-2} \tag{54}$$

Using the above-mentioned magnitudes and considering the corresponding initial and boundary conditions, the concentration and pressure distributions can be calculated by solving the equation system (28) and (29). Equation (28) is consisted of information about different transport mechanisms which can be reformulated as follows:

$$\frac{\partial c}{\partial t} =$$

$$\text{Source term:} \quad \frac{A_1}{\rho^{\mathrm{f}}}[c(1-c)]+ \tag{55}$$

$$\text{Diffusion term:} \quad \frac{D}{\rho^{\mathrm{f}}}[\mathrm{div}(\mathrm{grad}c)]+ \tag{56}$$

$$\text{Migration term:} \quad \frac{zFD}{\rho^{\mathrm{f}}R\theta}[\mathrm{grad}c \cdot \mathrm{grad}\phi + c\ \mathrm{div}(\mathrm{grad}\phi)]+ \tag{57}$$

$$\text{Convection term:} \quad \frac{1}{n^{\mathrm{f}}K}\left(\mathrm{grad}p - \rho^{\mathrm{fR}}\mathbf{g}\right) \cdot \mathrm{grad}c \tag{58}$$

The above-mentioned coefficients in front of each term can be substituted by a single representative coefficient and the influence of each process can be easily investigated by changing the corresponding coefficient. To do

so, dimensionally consistent coefficients λ^* with the unit s^{-1} can be defined, as follows:

$$\lambda_S = \frac{A_1}{\rho^{\mathrm{f}}} = \lambda_S^* \tag{59}$$

$$\lambda_D = \frac{D}{\rho^{\mathrm{f}}} = \lambda_D^* L^2 \tag{60}$$

$$\lambda_M = \frac{zFD}{\rho^{\mathrm{f}} R\theta} = \lambda_M^* \frac{L^2}{\Phi} \tag{61}$$

$$\lambda_C = \frac{1}{K} = \frac{1}{\lambda_C^* \rho_0} \tag{62}$$

In these equations, L is the characteristic length and chosen as $L = 1$ m.

In the following, three different examples are discussed. In these examples, only the steady state of the ion concentration is considered.

3.1 Convection-dominant process

In the first example, the process is mainly driven by convection ($\lambda_C \gg \lambda_D$). The problem is solved once by considering constant geometrical parameters (without back-coupling) and once by considering the changes in geometrical parameters (with back-coupling), the results of which are shown in Fig. 4.

As it is expected, the geometry changes have an influence on the coating process in a convection-dominant process. The coating of the foam reduces the pore space and, as a consequence, reduces the permeability. This leads to a reduction in the flow velocity. According to Darcy's law (see eq. 22), velocity has a direct relation with pressure gradient and lower velocity leads to lower pressure gradient, which can be noticed in Fig. 4b. With the reduction of flow velocity, the concentration of available ions in the electrolyte will reduce accordingly (Fig. 4a).

The transient concentration response for this example is presented in Fig. 5. In these graphs, the green line is the initial state of variables and the red line is the last time step. The effect of flow velocity reduction due to permeability reduction is illustrated in these figures clearly. Taking a glance at Fig. 5a, it can be seen that the flow velocity remained constant in all the time steps since the permeability is assumed to be constant during the deposition time. The trends in Fig. 5b show that the process has become slower by time as a result of the reduction of permeability in each time step.

3.2 Diffusion-dominant process

In the second example, a diffusion-dominant process is considered ($\lambda_D \gg \lambda_C$). Figure 6 shows the concentration and pressure results for such a process. As mentioned before, due to the permeability reduction, the velocity is reduced which, based on Darcy's law, leads to a decrease in pressure gradient (Fig. 6b). However, a diffusion-dominant process is driven mainly by the concentration gradient, and hence, the velocity changes have no considerable effects on the concentration changes. Therefore, as it is shown is Fig. 6a, in a diffusion-dominant process the concentration responses are almost independent of back-coupling calculations.

3.3 Influence of diffusion and convection

The last example deals with the influence of diffusion and convection on the concentration trend and compares three cases: when the diffusion is dominant, when the convection is dominant and when both mechanisms have the same magnitude of effect. Figure 7 shows the steady state of the ion concentration in these cases. The comparison is made once when the diffusion is constant and the change in ratio only happens through changes in the convection coefficient (Fig. 7a), and once with the constant convection and varying diffusion coefficient (Fig. 7b).

Comparing the results shown in Fig. 7, one can notice the dominance of convection influence on the process over the diffusion. It is evident from Fig. 7a that the change in the convection coefficient, i.e. flow velocity, leads to noticeable changes in the concentration rate. However, by doing a comparable investigation on the

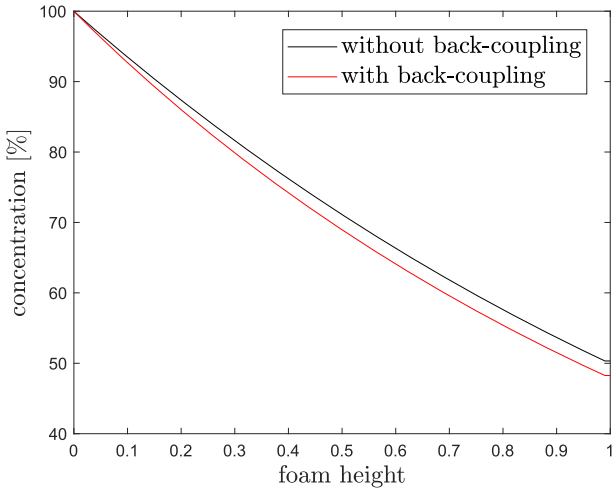

a Concentration distribution

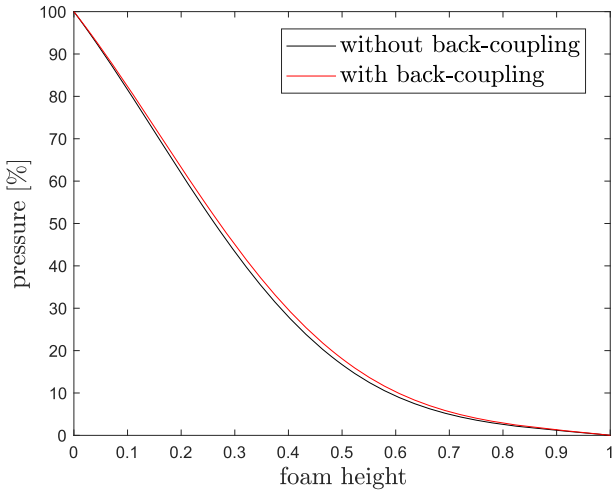

b Pressure distribution

Fig. 4 Comparison of steady-state responses of **a** concentration and **b** pressure with and without back-coupling calculations, in a convection-dominant process

diffusion coefficient, the changes in results are negligible (Fig. 7b). Also comparing the magnitude of ratios, it is apparent that a smaller variation in convection coefficient leads to much noticeable changes in concentration. To obtain a specific concentration change due to variation in diffusion coefficient, the variation should be of higher orders.

Finally, using the mentioned magnitudes in Tables 1 and 2, and considering the initial and boundary conditions, the transient response of the equation system (28) and (29) are presented in Fig. 8.

In the presented graphs in Fig. 8, the green line is the initial state of variables and the red line is the last time step. As shown in Fig. 8a, the concentration of available nickel ions in the electrolyte reduces during time until it converges to a steady state which means that the ions are either deposited on the struts or left the foam through the outlet. Moreover, the trends suggest that at the inlet of the foam, the concentration of ions are considerably higher than for the areas within the foam. This behaviour has also been observed in the experiments [9,13]. On the other hand, Fig. 8b predicts the behaviour of pressure. From a physical point of view, it is expected that when the process reaches to a steady state, the pressure changes show a semi-linear behaviour, which is demonstrated clearly in Fig. 8b.

The back-coupling calculation related to the changes of permeability is shown in Fig. 9.

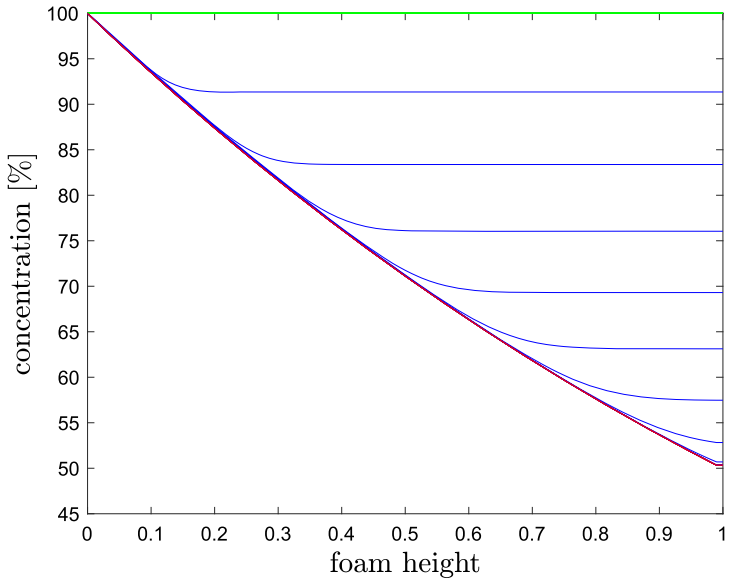

a Without back-coupling

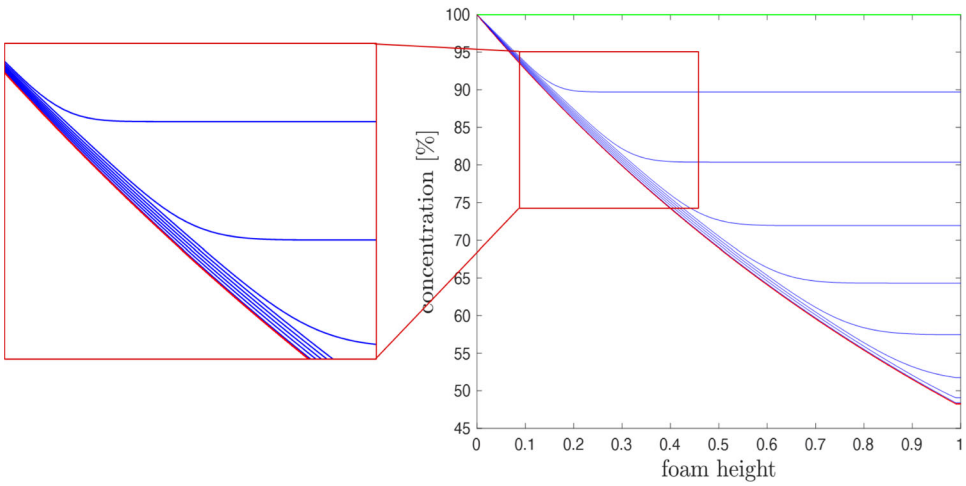

b With back-coupling

Fig. 5 Transient concentration response in a convection-dominant process **a** without and **b** with the back-coupling calculations

With the start of the coating process, the permeability of the foam reduces accordingly. Since the coating thickness is higher at the inlet of the foam, the permeability is smaller in this area than in the middle part of the foam.

The purpose of this investigation was to show some of the many potentials of the proposed model. This model offers the possibility to investigate the influence of different parameters on the results and to show the share of each transfer mechanisms in the coating process separately. All the results shown so far were computed considering a constant coefficient for migration and source term. The model can be used for further investigations of the influence of these mechanisms on the final results. In addition, the definition of the constitutive equations for the production term and the fluid density gives three more controlling parameters to adjust the model in order to obtain physically meaningful results. Moreover, the calculated reduced ion concentration as shown in Fig. 8a is partly due to the deposition and partly related to the ions that left the volume element with the flow of electrolyte. To be able to distinguish the deposited ions, the production term will be used, which finally would lead to the prediction of the coating thickness. Furthermore, differences

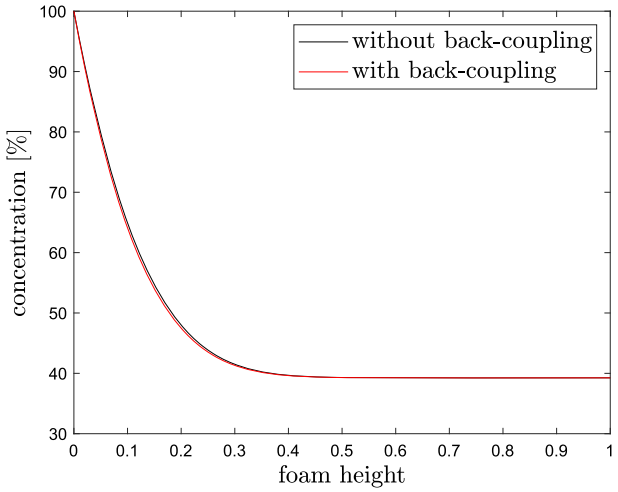

a Concentration distribution

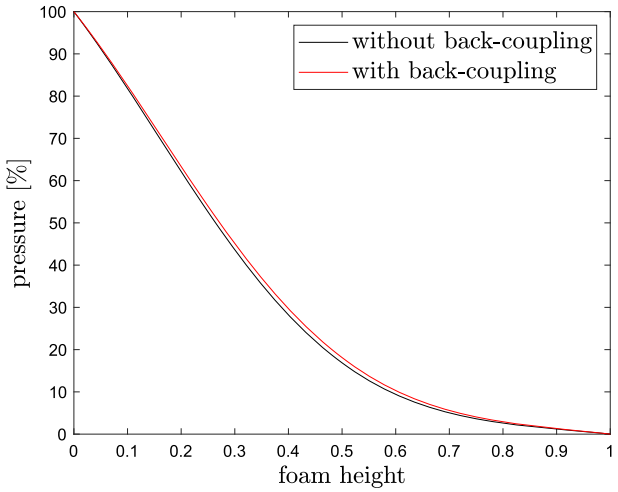

b Pressure distribution

Fig. 6 Comparison of steady-state responses of **a** concentration and **b** pressure with and without back-coupling calculations, in a diffusion-dominant process

to the experiment may be used to further modify the model by using a Robin boundary condition instead of Neumann boundary condition to consider the influence of convection and diffusion.

4 Conclusion and future work

This study proposes a method to model the coating process of polyurethane foams with nickel via electrodeposition. The problem is investigated in the framework of continuum mechanics for mixtures and the main transport mechanisms, namely diffusion, convection and migration, have been taken into account. In this regard, the governing system of equations for this problem has been derived using the fundamental balance equations of mass and momentum for each constituents and the mixture as a whole. Considering simplifying assumptions and defining suitable constitutive equations for the secondary unknowns, a closed system of equations is obtained which results to the calculation of time derivative of concentration and pressure distribution throughout the foam. The proposed model is able to investigate the influence of different processes on the concentration distribution. Furthermore, by introducing a back-coupling technique, the parameter changes during the process and its influences on the deposition have been taken into account.

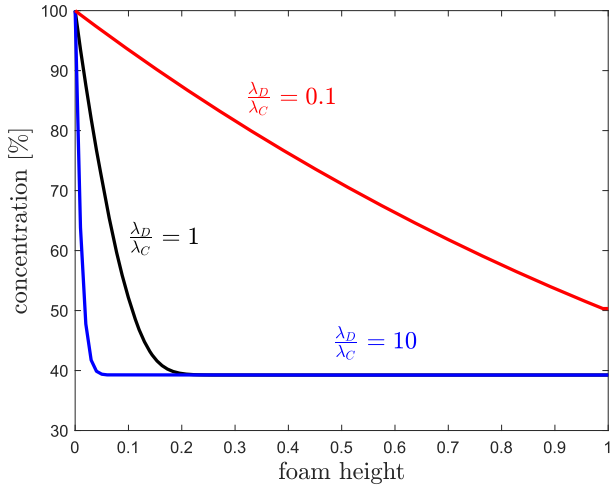

a

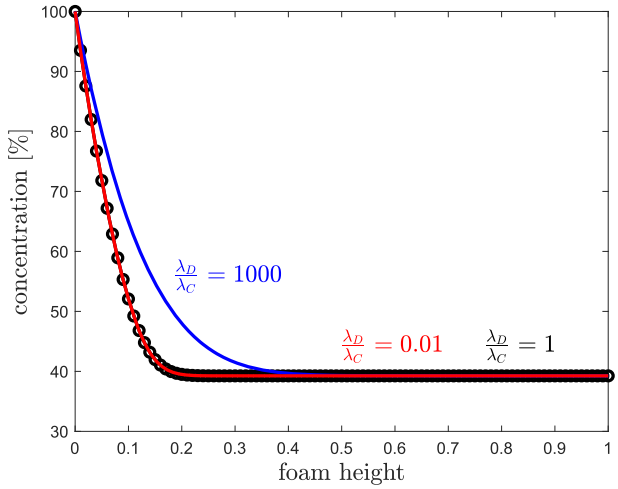

b

Fig. 7 Influence of $\frac{\lambda_D}{\lambda_C}$ on concentration at steady state with **a** constant diffusion coefficient and **b** constant convection coefficient

Finite difference method has been used to solve the equations. The results obtained from the first simulations for a one-dimensional domain exhibit a promising ability of the model to describe the experimental observations. This study can be developed in future and investigate the coating process with more details and from different aspects. Therefore, with the help of these data and performing a parameter study, the coating process can be optimized and suitable conditions to obtain a homogenized coating all over the foam can be suggested.

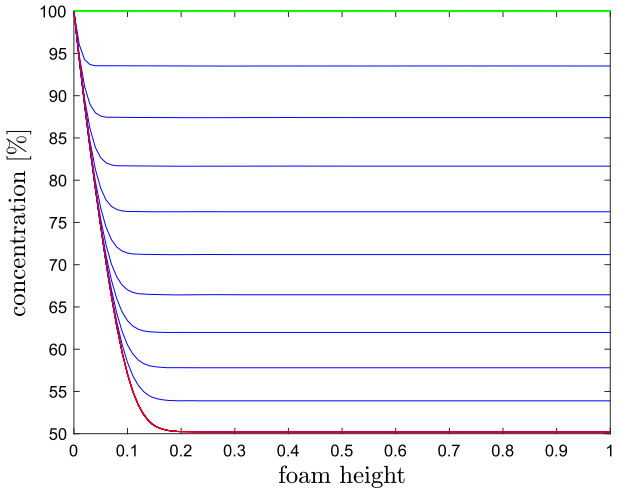

a Concentration distribution

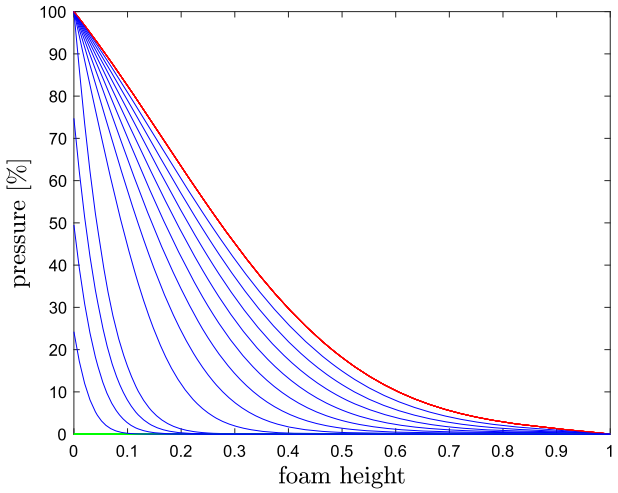

b Pressure distribution

Fig. 8 Transient distribution of **a** concentration and **b** pressure within the foam height in the direction of flow

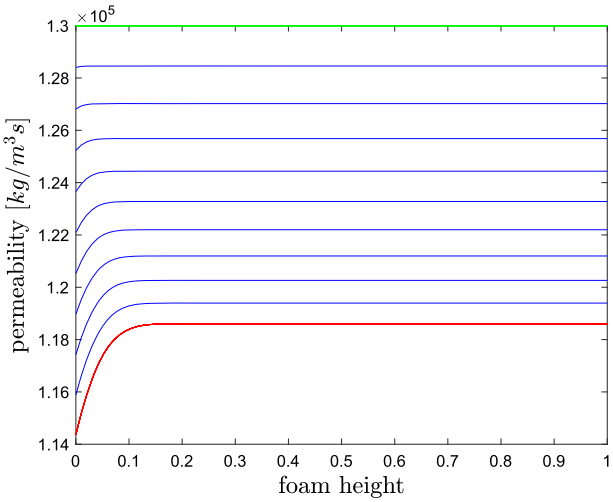

Fig. 9 Back-coupling results of permeability evolution within the foam height in the direction of flow

Author contribution N.G. wrote the main manuscript, developed the model and obtained the results. P.S. reviewed the manuscript and acted as a second supervisor. A.J. provided the research idea and the information about the experiments. S.D. was the main supervisor and reviewed the manuscript.

Funding Open Access funding enabled and organized by Projekt DEAL. This work was supported by the German Science Foundation (DFG) under the grants DI430/35-1.

Data availability The datasets used and analysed during the current study are available from the corresponding author on reasonable request.

Declarations

Conflict of interest The authors declare no conflict of interest.

References

1. Banhart, J.: Manufacture, characterisation and application of cellular metals and metal foams. Prog. Mater Sci. **46**(6), 559–632 (2001)
2. Duarte, I., Peixinho, N., Andrade-Campos, A., Valente, R.: Special issue on cellular materials. Sci. Technol. Mater. **30**(1), 1–3 (2018)
3. Liu, P.S., Chen, G.F.: Porous Materials: Processing and Applications. Elsevier, Amsterdam (2014)
4. Gladysz, G.M., Chawla, K.K.: Voids in Materials: from Unavoidable Defects to Designed Cellular Materials. Elsevier, Amsterdam (2020)
5. Jung, A., Diebels, S.: Micromechanical characterization of metal foams. Adv. Eng. Mater. **21**(8), 1900237 (2019)
6. Jung, A., Diebels, S.: Hybrid metal foams: experimental observations and phenomenological modelling. Technische Mechanik-Eur. J. Eng. Mech. **34**(1), 12–22 (2014)
7. Jung, A., Natter, H., Diebels, S., Lach, E., Hempelmann, R.: Nanonickel coated aluminum foam for enhanced impact energy absorption. Adv. Eng. Mater. **13**(12), 23–28 (2011)
8. Jung, A., Diebels, S.: Synthesis and mechanical properties of novel Ni/Pu hybrid foams: a new economic composite material for energy absorbers. Adv. Eng. Mater. **18**(4), 532–541 (2016)
9. Kunz, F., Jung, A.: Investigation of the structural coating homogeneity in open-porous Nickel/Polyurethane hybrid foams produced by flow-controlled electrodeposition. Adv. Eng. Mater. **24**(11), 2200262 (2022)
10. Euler, K.J.: Die nderung der Stromverteilung in porösen positiven Elektroden von Akkumulatoren und galvanischen Primärzellen während Ladung und Entladung. Electrochim. Acta **13**(7), 1533–1549 (1968)

11. Euler, K.J.: Stromverteilung in und auf porösen Elektroden. Chem. Ing. Tec. **37**(6), 626–631 (1965)
12. Euler, K.J.: Spatial current distribution in non-isotropic conductors (with implication for porous electrodes). Electrochim. Acta **18**(5), 385–387 (1973)
13. Grill, C., Fries, M., Jung, A., Diebels, S.: Numerical and experimental investigations of the electrodeposition process on open porous foams, determination of the parameter influence on the coating homogeneity. Int. J. Heat Mass Transf. **180**, 121791 (2021)
14. Jung, A., Koblischka, M.R., Lach, E., Diebels, S., Natter, H.: Hybrid metal foams: mechanical testing and determination of mass flow limitations during electroplating. Int. J. Mater. Sci. **2**(1), 97–107 (2012)
15. Hughes, M.R., Strussevitch, N., Bailey, C., McManus, K., Kaufmann, J.G., Flynn, D., Desmulliez, M.P.Y.: Numerical algorithms for modelling electrodeposition: tracking the deposition front under forced convection from megasonic agitation. Int. J. Numer. Meth. Fluids **64**, 237–268 (2010)
16. Joekar-Niasar, V., Schreyer, L., Sedighi, M., Icardi, M., Huyghe, J.: Coupled processes in charged porous media: from theory to applications. Transp. Porous Media **130**(1), 183–214 (2019)
17. Grill, C., Jung, A., Diebels, S.: Modelling and simulation of the coating process on open porous metal foams. PAMM **18**(1), 201800254 (2018)
18. Grill, C., Jung, A., Diebels, S.: Investigation of the electrodeposition parameters on the coating process on open porous media. PAMM **19**(1), 201900106 (2019)
19. Ghiasi Shirazi, S.N.: Numerical Modelling of Ni/Pu Hybrid Foams Coating Process. PhD thesis, Universität des Saarlandes, Saarbrücken (2024). https://doi.org/10.22028/D291-42475
20. Bowen, R.M.: Theory of Mixtures. In: Eringen, A.C. (ed.) Continuum Physics III, pp. 1–127. Academic Press, New York (1976)
21. Ehlers, W., Bluhm, J.: Porous Media: Theory, Experiments and Numerical Applications. Springer, Berlin- Heidelberg (2002)
22. Truesdell, C., Toupin, R.: The classical field theories. In: Flügge, S. (ed.) Principles of Classical Mechanics and Field Theory/Prinzipien der Klassischen Mechanik und Feldtheorie, pp. 226–858. Springer, New York (1960)
23. Miyan, M., Pant, P.K.: Flow and diffusion equations for fluid flow in porous rocks for the multiphase flow phenomena. Am. J. Eng. Res. **4**(7), 139–148 (2015)
24. Ehlers, W.: Darcy, Forchheimer, Brinkman and Richards: classical hydromechanical equations and their significance in the light of the TPM. Arch. Appl. Mech. **92**(2), 619–639 (2022)
25. Jasielec, J.J.: Electrodiffusion phenomena in neuroscience and the Nernst-Planck-Poisson equations. Electrochem **2**(2), 197–215 (2021)
26. Cohen, H., Cooley, J.W.: The numerical solution of the time-dependent Nernst-Planck equations. Biophys. J . **5**(2), 145–162 (1965)
27. Hommel, J., Coltman, E., Class, H.: Porosity-permeability relations for evolving pore space: a review with a focus on (bio-) geochemically altered porous media. Transp. Porous Media **124**(2), 589–629 (2018)
28. Li, Z., Qiao, Z., Tang, T.: Numerical Solution of Differential Equations: Introduction to Finite Difference and Finite Element Methods. Cambridge University Press, Cambridge (2017)
29. Holmes, M.H.: Introduction to Numerical Methods in Differential Equations. Springer, New York- Heidelberg- Dordrecht-London (2007)
30. LeVeque, R.J.: Finite difference methods for differential equations. Draft version for use in AMath **585**(6), 112 (1998)
31. Ames, W.F.: Numerical Methods for Partial Differential Equations. Academic press, New York (2014)
32. Sato, H., Yui, M., Yoshikawa, H.: Ionic diffusion coefficients of Cs^{+}, Pb^{2+}, Sm^{3+}, Ni^{2+}, SeO_4^{2-}, and TcO_4^{-} in free water determined from conductivity measurements. J. Nucl. Sci. Technol. **33**(12), 950–955 (1996)